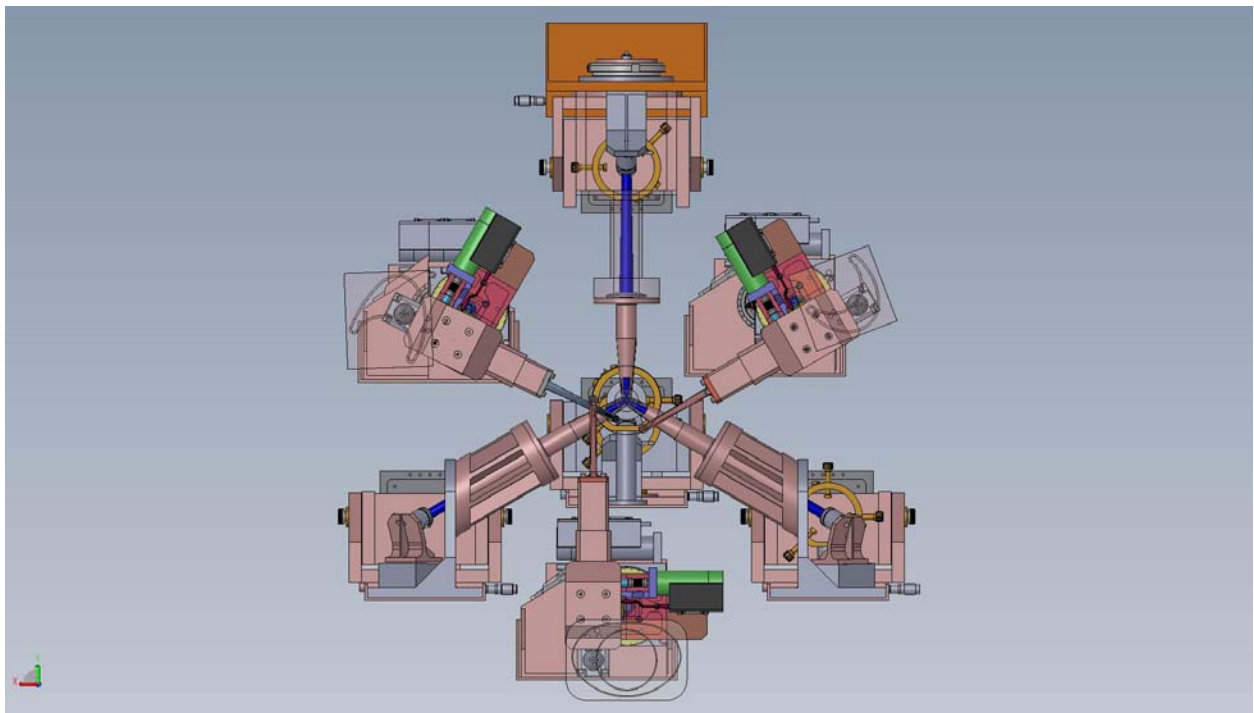




LGS Wavefront sensor sub-system preliminary design

KECK ADAPTIVE OPTICS NOTE xxx

November 21, 2009





1. Introduction and Overview of concept

This document describes the preliminary design of the Laser Guide Star Wavefront Sensors (LGSWFS) for Keck’s Next Generation Adaptive Optics (NGAO) system.

Following the conceptual design review a Build-to-Cost (B2C) review was conducted which led to considerable changes in the system architecture, in particular to the LGS WFS architecture¹. Firstly, the deployable quincunx asterism was de-scoped to a fixed LGS asterism with one on-axis LGS and three fixed symmetrically located LGS’s located at 10” radius. The FoV of the three movable PnS LGS used to sharpen the NGS TT stars was reduced from 150” to 120”. To further simplify the architecture and ease implementation, the wavefront measurements from these TT stars and the corresponding LGS WFS will be used to run separate AO systems that sharpen the TT stars but don’t contribute to the tomographic reconstruction.

Another significant change is the implementation of the LGS differential TT on the downlink rather than stabilize the laser beacon on sky. This provides for better control bandwidth as the time-delay between a measurement and TT correction is much smaller by the cycle time of light traveling up and down to the sodium layer.

The LGSWFS team has tried to design a simple, cheap and transmission efficient system that fulfills the requirements.

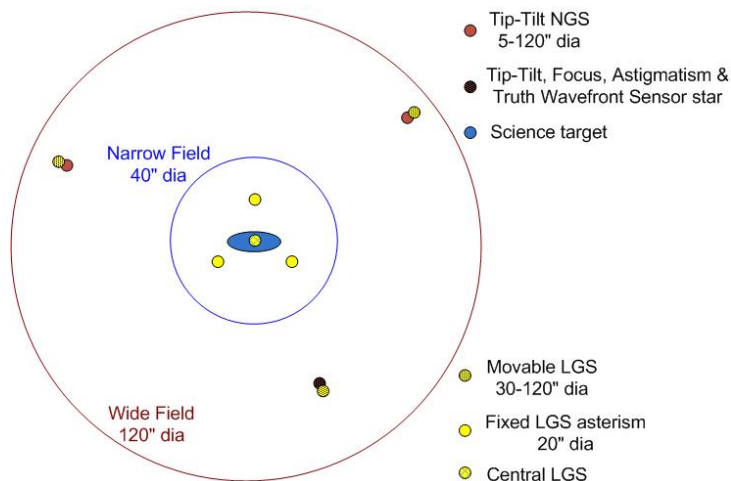


Figure 1- LGS “3+1” tomography asterism for the science field and three point and shoot lasers for image sharpening of the tip-tilt stars



Context diagram

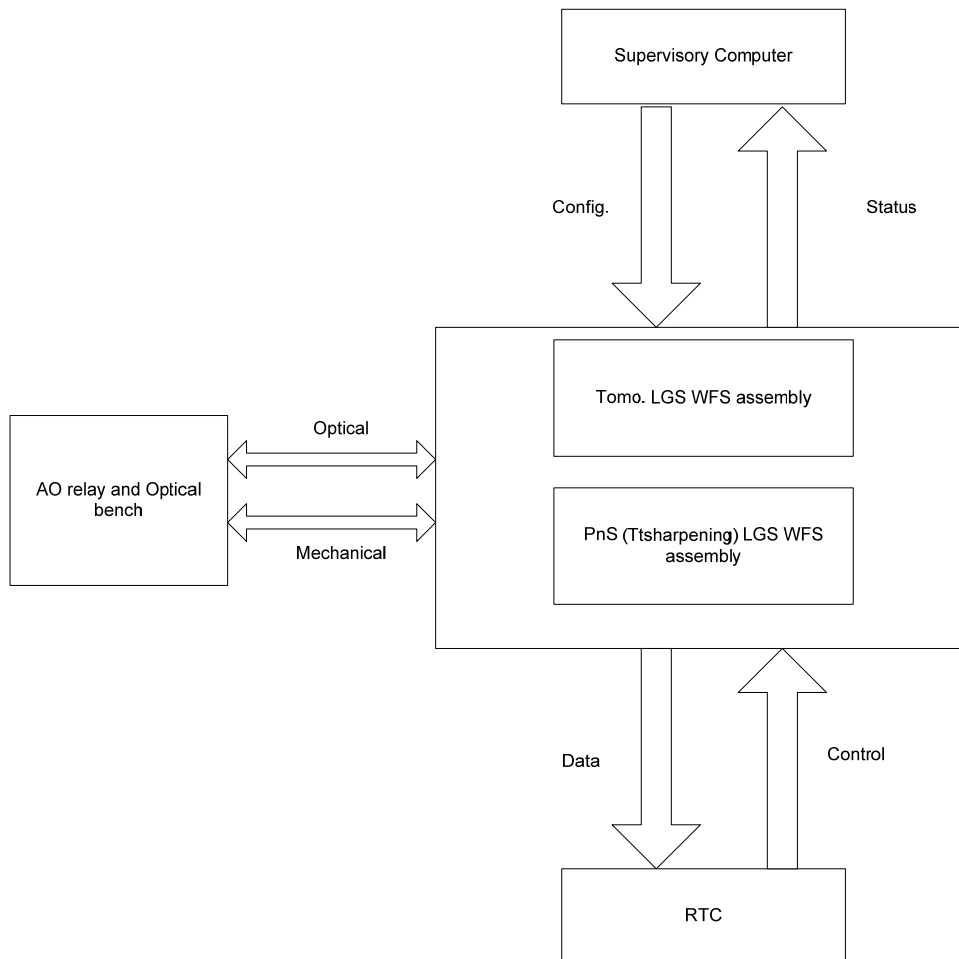


Figure 2- Context diagram of the LGSWFS showing the basic mechanical, optical and control interfaces to the AO system

Figure 2 is a basic context diagram of the LGSWFS assembly showing the interfaces of the WFS subsystem with rest of the NGAO system. LGSWFS make centroid measurements using 589 nm light from the AO system and send this data to the RTC to drive the LODM, HODM the 32x32 actuator MEMS DM's in the TT(FA) WFS channels. At the same time the RTC also controls the downlink TT mirror position. The supervisory control computer helps deploy the PnS sensors and acquire the LGS light and configure the LGSWFS cameras (bias levels, gains, frame rate etc.). The LGSWFS subsystem will provide a status signal to the supervisory computer as a status monitor. Figure 3 shows a more detailed schematic of the LGSWFS assembly. Shown in the figure are a single PnS WFS channel with a deployable theta-phi pick-off mechanism with a fast downlink TT mirror, a slow TT mirror to register the lenslet and HODM pupils at each point in the field of regard and a rotary mechanism that rotates the WFS channel to keep the orientation of the lenslet and HODM acutators constant by undoing rotation introduced by the theta-phi mechanism.



2. Reference documents

- 2.1. [KAON 551 Wavefront Sensor System Conceptual Design Report](#)
- 2.2. [511 System Design Manual v2.1 \(doc\)](#), dated March 30th, 2008
- 2.3. [Preliminary Design Manual](#) (as of November 12th, 2009)
- 2.4. [685 Opto-mechanical Design Document](#)
- 2.5. [666 Fixed Pupil Mode](#)
- 2.6. [Flowdown Error Budget](#)

3. AO relay path to LGSWFS input

The Laser guide star light path is shown in Figure 5, the laser light traverses through the K mirror and the fold followed by the 1st AO relay OAP, after which it is incident on the DM. Following the DM it is folded by a notch dichroic and a 1m focal length plano-convex lens, with the convex surface being a parabola, focuses the beam to a tilted focal plane. The Laser Guide Star Wavefront Sensor assembly is located after the focus created by the AO relay. Figure 4 shows the mechanical layout of the NGAO system indicating the location of the LGSWFS assembly.

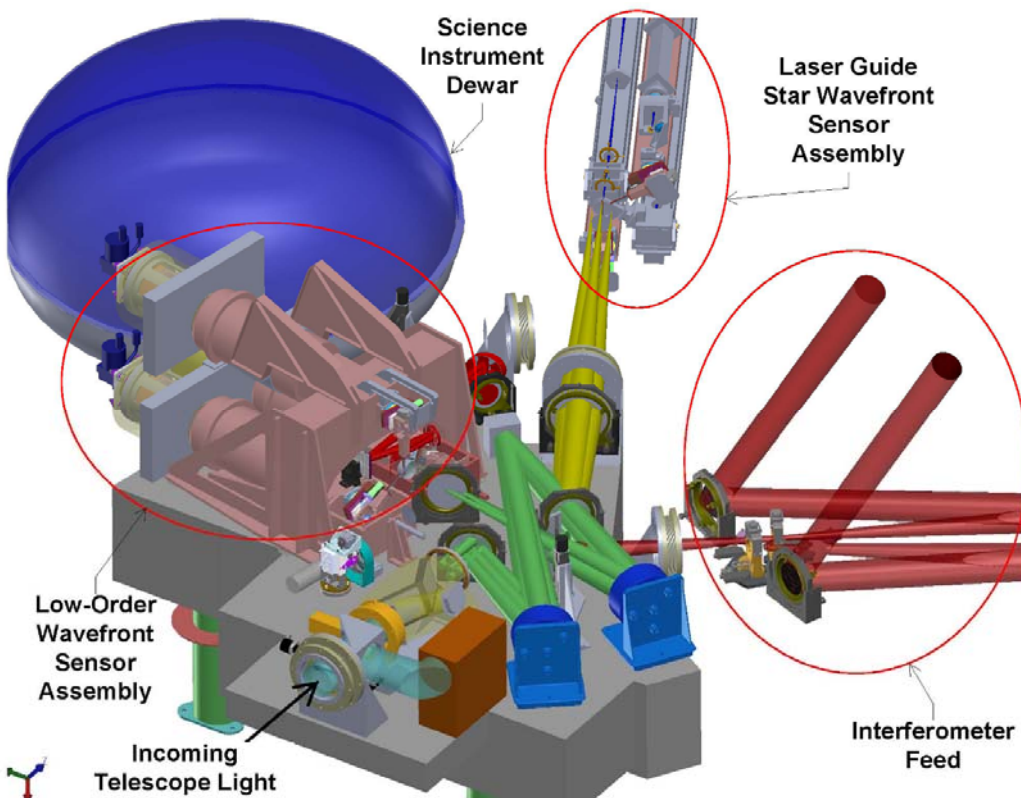


Figure 4 - NGAO optical layout showing the location of the LGSWFS assembly WRT rest of the system (pic. courtesy C. Lockwood, UCO Lick)

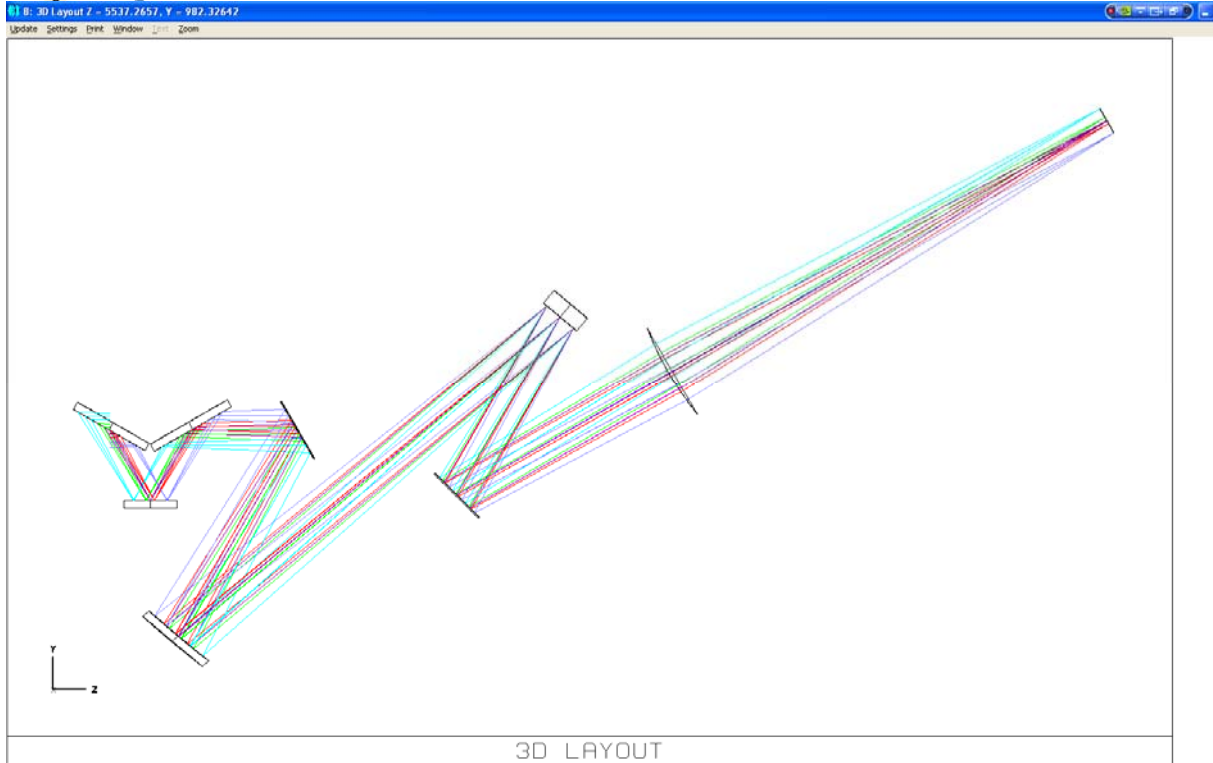


Figure 5 - Laser guide star light path starting from the K mirror to the LGSWFS pick-off focal plane.

Figure 6 shows the spot diagram from the AO relay at 90 Km Na layer distance. The central fixed LGS spots delivered by the AO relay have RMS radii between 25 and 45 μm at the LGS pick-off plane. The PnS LGS spots sizes range between 130 and 150 μm RMS radius. The working F# at the LGS pick-off is 13.56 at 22 degrees off zenith and 720 μm at the LGS pick-off plane corresponds to an arcsec on sky as per Zemax model of the NGAO Optical Relay. It is useful to note that the LGS focal plane delivered by the AO system is both curved and tilted. The curvature of the focal plane varies between 883 mm and 2604 mm as the distance to Na-layer varies from 90 to 180 Km.

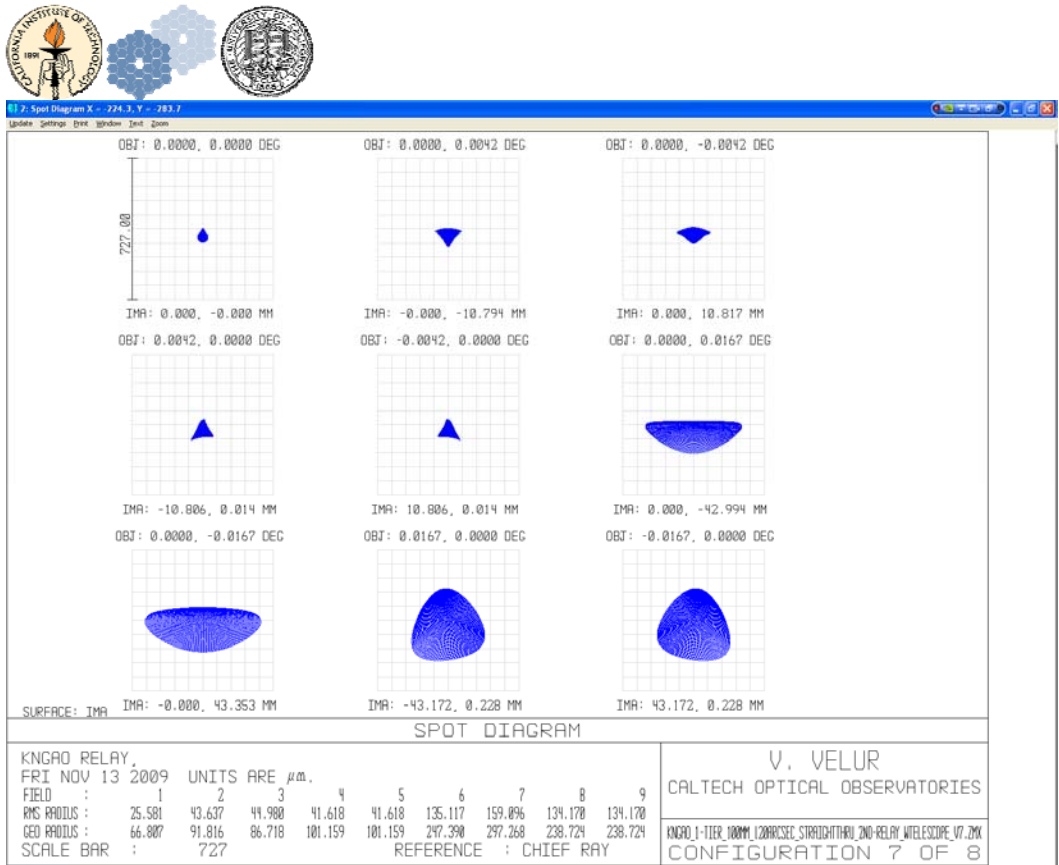


Figure 6- LGSWFS spots when the telescope is pointing at zenith. The fixed LGS spots at the LGSWFS pick-off focal plane is 25-45 μm (RMS) radius while the PnS LGSWFS spots are as big as 160 μm (RMS) at the edge of the field.

To understand the effect rather large spot sizes delivered by the AO relay as seen by the most affected PnS LGS WFS sub-apertures, we swap the Keck primary mirror with movable aperture that is $1/31^{\text{st}}$ of the primary mirror and de-center this aperture to the extreme points of the primary mirror to look at the resulting spots to understand what happens at the Shack-Hartmann sub-apertures. One can see RMS radii of almost 6 μm at the edge of the field as is shown by Figure 7 and Figure 8.

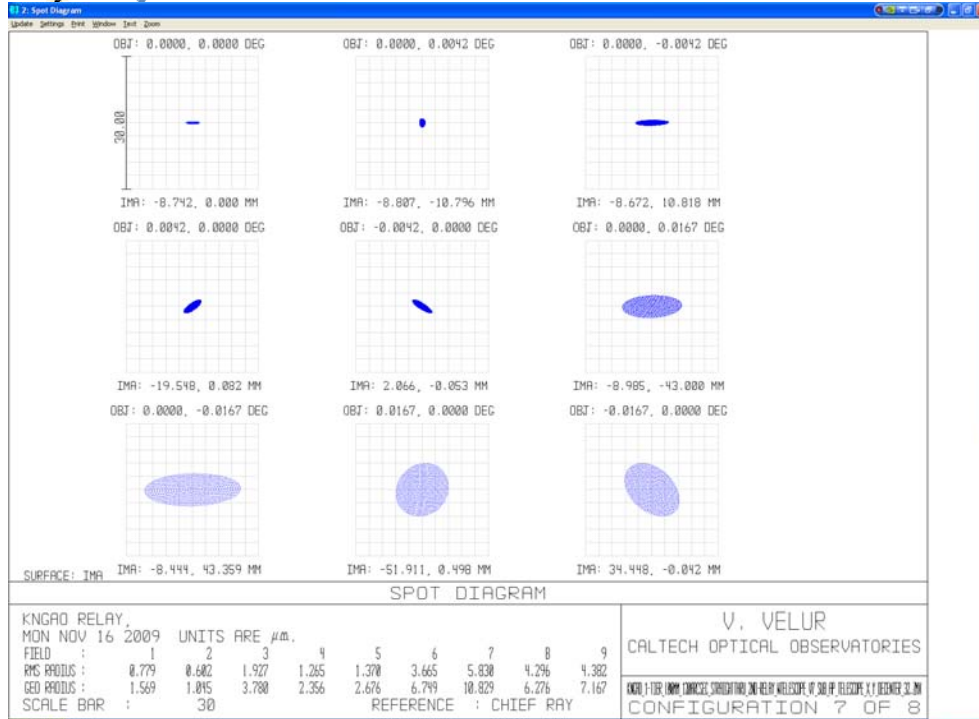


Figure 7 LGS spots as seen by a single PnS LGSWFS sub-aperture. The spots diagram was generated by creating a de-centered aperture that is 1/31st the size of the Keck primary mirror and making the entrance pupil the size of a single sub-aperture. The aperture parameter in the Surface Property Menu was set to the primary mirror radius (5297.9 mm) to accommodate ray tracing. The worst case sub-aperture spots see a 6 μm (RMS) radius.

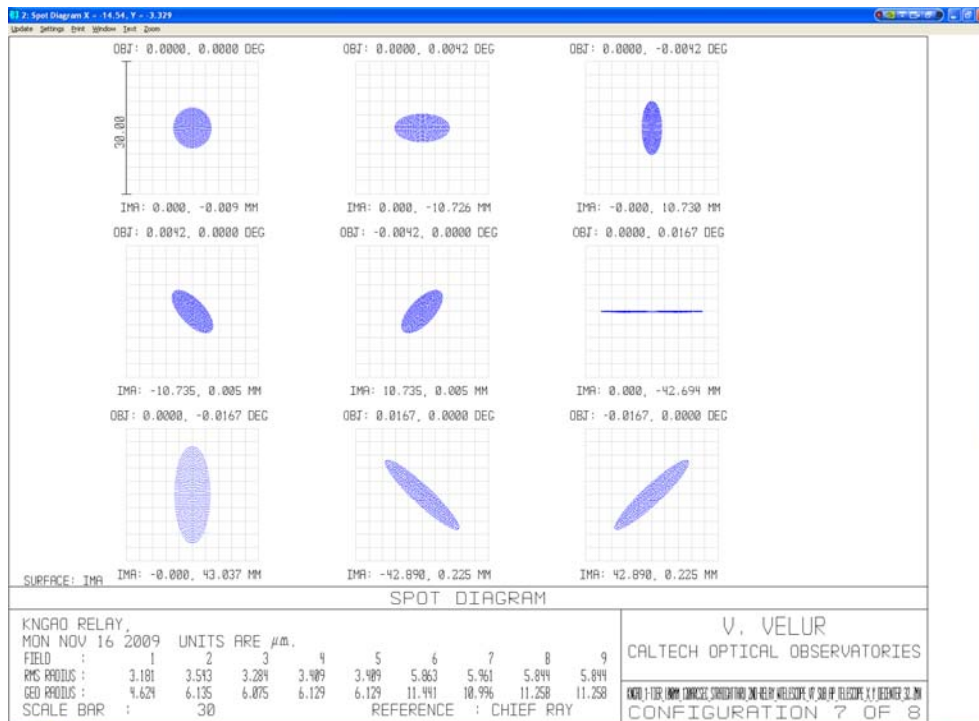


Figure 8 - LGS spots as seen by a PnS LGSWFS sub-aperture (de-centered in the orthogonal direction). Worst case sub-apertures are 6 μm (RMS) radius.



4. Requirements highlights

5. WFS Design

5.1.Relevant analysis for design

5.1.1. Pixel scale choice

From experience we know that characterizing and calibrating each sub-aperture of the 7 WFS for non-linearity is non-trivial and hence we choose the plate-scale to ensure that the sensor operates in its linear regime. Pixel scale is chosen based on the apparent spot size (sans charge diffusion). Figure 9, extracted from the EBS, shows the apparent spot size for the tomographic (left column) and PnS (right column). For the fixed LGS asterism, the 1D tilt error is 50 mas and the diffraction limited sub-ap spot size is 699 mas, so we choose $p=0.5$ from Table 1 to accommodate capture range and linear operating regime. For the variable asterism the 1D tilt error is 329 mas and the sub-ap diffraction limited spot size is 343 mas, so we choose $P=1.0$ for this sensor based on Table 1 to be able to measure ± 2.5 waves of tilt.

Detector size per subaperture	Pixel Size/ spot size (p)	Useful tilt range +/- waves	Departure from linearity
2x2	1.0-1.5	0.5	0.024
2x2		1.0*	.13*
4x4	0.5	1.5	0.019
4x4	0.67	2	0.085
4x4	1	2.5	0.19

* - nonlinear response

Table 1 - Dynamic range and linearity of Shack-Hartmann quad-cells (this is same as Table 5.3, Pg. 149 of Hardy). NGAO PnS LGS WFS's use a 4x4 pixel sub-aperture with $p=1$; while we choose a p of 0.5 for the fixed LGSWFS's.



Laser Guide Star Size Calculation		Laser Guide Star Size Calculation	
Finite Object Size		Finite Object Size	
Intrinsic guide star diameter	0.00 arcsec	Intrinsic guide star diameter	0.00 arcsec
Uplink formation of the beacon(s)		Uplink formation of the beacon(s)	
Perfect Uplink AO?	NO	Perfect Uplink AO?	NO
Inherent aberrations in the uplink beam:	0.90 arcsec	Inherent aberrations in the uplink beam:	0.90 arcsec
Beam movement contribution to uplink	0.27 arcsec	Beam movement contribution to uplink	0.27 arcsec
Residual seeing contribution to uplink	0.47 arcsec	Residual seeing contribution to uplink	0.47 arcsec
Diameter of point source laser at Na layer:	1.02 arcsec	Diameter of point source laser at Na layer:	1.02 arcsec
Seeing		Seeing	
Natural seeing FWHM at GS wavelength	0.46 arcsec	Natural seeing FWHM at GS wavelength	0.46 arcsec
Subaperture Tip/Tilt corrected FWHM	0.36 arcsec	Subaperture Tip/Tilt corrected FWHM	0.39 arcsec
AO-compensated FWHM	0.06 arcsec	AO-compensated FWHM	0.06 arcsec
Contribution due to seeing	0.36 arcsec	Contribution due to seeing	0.39 arcsec
Elongation		Elongation	
Distance from LLT to telescope axis:	0.00 m	Distance from LLT to telescope axis:	0.00 m
Use Max. Elongation?	NO	Use Max. Elongation?	NO
Avg. Elongation	1.39 arcsec	Avg. Elongation	0.93 arcsec
Contribution to FWHM due to elongation	0.49 arcsec	Contribution due to elongation	0.93 arcsec
System Aberrations		System Aberrations	
Aberations in AO thru to WFS	0.25 arcsec	Aberations in AO thru to WFS	0.25 arcsec
Atmospheric Dispersion		Atmospheric Dispersion	
ADC in HOWFS?	NO	ADC in HOWFS?	NO
RMS blurring due to atmospheric dispersion	0.000 arcsec	RMS blurring due to atmospheric dispersion	0.000 arcsec
Total size of detected return beam:	1.21 arcsec	Total size of detected return beam:	1.45 arcsec
Sensing Approach		Sensing Approach	
Pyramid WFS?	NO	Pyramid WFS?	NO
Charge Diffusion		Charge Diffusion	
Charge Diffusion	0 pixels	Charge Diffusion	0.00 pixels
Contribution due to Charge Diffusion	0.00 arcsec	Contribution due to Charge Diffusion	0.00 arcsec
Subaperture Diffraction		Subaperture Diffraction	
Lambda/d (for sensing)	0.71 arcsec	Lambda/d (for sensing)	0.36 arcsec
Spot size used for centroiding	1.41 arcsec	Spot size used for centroiding	1.49 arcsec

Figure 9 apparent spot size measurement at the detector due to various effects for the fixed tomographic LGS WFS spots (left) and that of deployable PnS (TT sharpening) LGS WFS spots (right). Charge diffusion term is set to 0 to come up with an estimate of the detector platescale.

5.1.2. Downlink TT mirror choice

To determine the TT mirror of choice, we need to specify the resolution and the throw required for the mirror given the bandwidth requirement from the requirements database.

$$\text{Pupil de-magnification at the TT mirror} = 10.949 \text{ m} / (12.5 \text{ mm} / 1000 \text{ mm/m}) = 875.92$$

TT resolution on sky = 1 milliarcsec (say)

[The RMS 1D tilt error is 95 milliarcsec (c.f. EBS Version 1.48)]

$$\text{Hence, TT mirror resolution} = 0.001 \text{ (arcsec)} * 875.92 = 0.875 \text{ arcsec} = 4.2 \text{ microradians}$$

$$\text{Capture need, say is, } 0.5 \text{ arcsec (on sky angle)} = 0.5 * 875.92 \text{ ''} / 206265 \text{ (''/rad)} = 2.12 \text{ millirad}$$



Based on the resolution and the capture range we choose the following mirror from Physik Instrumente's catalog:

<http://www.physikinstrumente.com/en/products/prspecs.php?sortnr=300700>

S-330.8SL has 10 mrad of tilt travel with 0.5 microrad (0.12 milliarcsec resolution on sky) open-loop resolution is the mirror of choice. The mirror has a resonance frequency of 1 KHz with a 1" diameter optic with ¼" thickness.

5.1.3. The effect of using a single global focusing stage with no individual stages for the 7 LGSWFS channels:

Individual LGS WFS channels see differential focus due to two effects; viz. change in ROC of the LGS focal plane with change in distance to the sodium layer (c.f. Table 2) and due to the finite size of the LGS asterism on sky. The physical distance between the innermost and outermost laser beacons on-sky vary with zenith angle as shown in Figure 10; this effect is quantified in Table 3. Both effects, though not negligible, are entirely deterministic given the position and geometry of the LGS asterism and so the defocus can be calibrated away by the RTC. So the preferred design choice is to use a single focusing stage for the entire LGSWFS assembly.

Sodium layer altitude	ROC of focal plane (from Zemax)	Focal plane size	Sagitta
90 km	883.2 mm	7.27 mm	0.0299 mm
180 km	2064 mm	7.27 mm	0.0128 mm
		difference in sag =	0.0171 mm

Table 2 - Radii of curvature of the LGS focal plane as delivered by the NGAO optical relay at 90 and 180 km Na layer object distance and the change in focus due to the changing ROC.

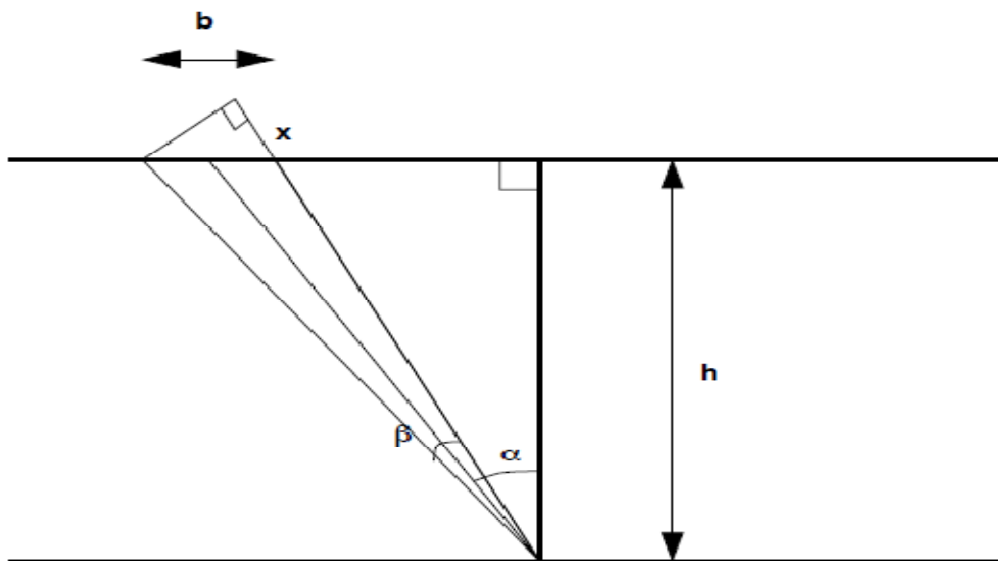


Figure 10 - Schematic showing defocus between the innermost and outermost LGS due variation in physical distance of those with zenith angle.



$\alpha = 1.221$ degrees (at 70 degrees off zenith pointing)

$\beta = 7.2722 * 10^{(-2\%)} \text{ deg.}$

$b = h/\cos(\alpha) * \beta$

$x = b*\tan(\alpha)$

Where, α is the telescope DEC angle WRT zenith.

β is the angle subtended by the beacons onto the laser launch telescope

h is the Na layer altitude at zenith (90 km)

b is the physical distance between the innermost and outermost beacon at the Na layer.

X is the object distance shift between the innermost and outermost laser beacon.

Guide star radius	defocus error due to geometry of the asterism (um)	Error in waves
10	17	0.0778 waves
50	68	0.311 waves

Table 3 - shows the error due to change in focus between the innermost and outermost LGS with zenith angle. For reference $\lambda/4$ depth of focus is 147 nm of WFE and 219 um of defocus (as given by $2*\lambda*F/\#^2$).

5.1.4. LGS WFS relay performance specification

Internal WFS aberration allocation is 0.25" (FWHM). The LGS spots delivered by the OSM are 3 and 8 times smaller in (RMS) radii than the input spots from the AO relay for the fixed and deployable LGSWFS's respectively. The OSM's contribution corresponds to an FWHM of ~ 0.05 arcsec. Hence, the LGSWFS relay performance needs to have: Spot size (RMS as indicated by Zemax) at the detector = Allocation (arcsec FWHM)/2.355 (FWHM/RMS) * 21 (um/pixel)/1.49 (arcsec/pixel) = $0.25/2.355*21/1.49 = \sim \underline{1.5 \text{ um}}$

5.1.5. Field stop specification

The FoV of the tomographic and PnS subapertures are 5.96 and 5.64 arcsecs respectively. A square- field stop that is 3.6 arcsecs on the edge will be positioned at the WFS focus to prevent crosstalk of LGS spots at the detector.

5.2. Optical design and performance

5.2.1. Fixed LGS WFS

5.2.1.1. Wavefront sensor design math

Pixel size/spot size = 0.5 (as per Table 1)

From the AO system optical design, 720 um is an arcsec.



Hence, 1.41" corresponds to 42 um (2*21 um detector pixels).

$$f_{\text{collimator}}/f_{\text{lenslet}} * 1/m = \text{Plate scale at the input of the sensor(um/asec)/ Detector plate scale (um/asec)}$$

$$= 720/29.78 = 24.4064 \text{ (720 is the \# obtained from Zemax); we choose } f_{\text{collimator}} = 80 \text{ mm from JML's catalog.}$$

We choose a commercial collimator instead of a commercial lenslet as the Fresnel Number (FN) of the lenslet is fixed and any (non-custom) commercial lenslet needs to have the exact same FN to be used in NGAO. The limited lenslet database didn't have any match for the required lenslet FN.

$$d_{\text{each lenslet}} = f_{\text{collimator}}/f\# * 1/(\# \text{ of sub-aps}) = 80/13.56 * (1/63) = 93.6 \text{ um (choose a 80 mm focal length lens).}$$

$$m = 0.084/0.0936 = 0.896$$

$$f2 = f_{\text{collimator}}/m * (29.78/720) = 80/0.89699 * (1/24.17145) = 3.68 \text{ mm (f/\# lenslet = 39.42)}$$

$$\text{lenslet array Fresnel \#} = (d_{\text{each lenslet}}/2)^2/(f*\lambda) = 1.01.$$

The FN term is an invariant and can be expressed as $1/(4*\lambda) * (D_{\text{telescope}}/\# \text{ of subaps}) * (\text{spot sep. in radians})$

The simplest possible tomographic LGSWFS with the least # of surfaces can be made with a best form singlet and a lenslet array directly imaging spots onto a detector without using a reimaging relayⁱⁱ. Such a design will have a lenslet pitch of 84 um and lenslet focal length of 2.97 mm with a 71.76 mm EFL collimator. The whole wave front sensor is compact and has only 4 surfaces with either the collimator or the lenslet serving as the detector window. Such a WFS was designed using a custom collimator and a custom lenslet. The design is available at http://www.oir.caltech.edu/twiki_oir/pub/Keck/NGAO/WFS/fixe_d_lgs_wfs_norelay.ZMX. The problem with the sensor is the complexity of alignment and procurement with no margin of error due to lack of degrees of freedom to adjust the lenslet spots onto the detector.

5.2.1.2. Fixed LGSWFS pick off design and performance

To accommodate mechanical packaging and keep the optical surfaces to a minimum, a 1:1 relay was chosen with a total length of 640 mm (Alex to add packaging constraints). Figure 11 and Figure 12 show the optical layout of the relay and spot diagrams they deliver. The relay has a FoV of 5" and is designed to be telecentric in order to not introduce any spurious tilts in the beam due to the incidence position of the LGS light on the pickoff. The spots sizes are 16 um RMS compared to 40 um RMS spots that the AO relay generated from the AO relay. The design for the pick off is available at http://www.oir.caltech.edu/twiki_oir/pub/Keck/NGAO/WFS/fixe_d_LGS_pick_off.ZMX

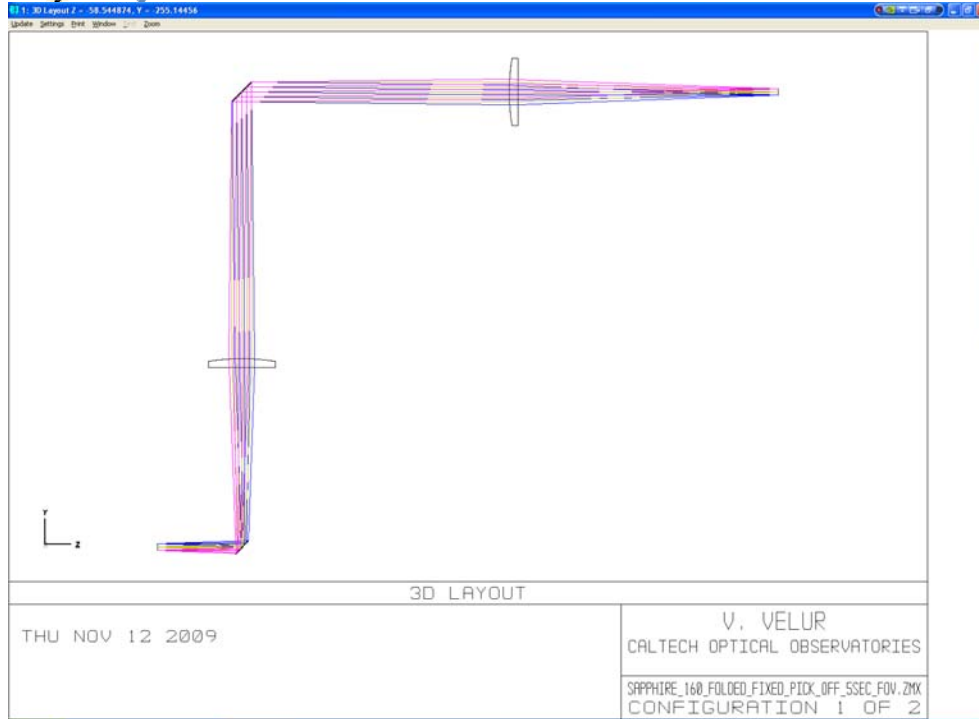


Figure 11 - Telecentric 1:1 fixed LGSWFS pick off relay. The total length of the relay is 640 mm (limited by packaging constraints).

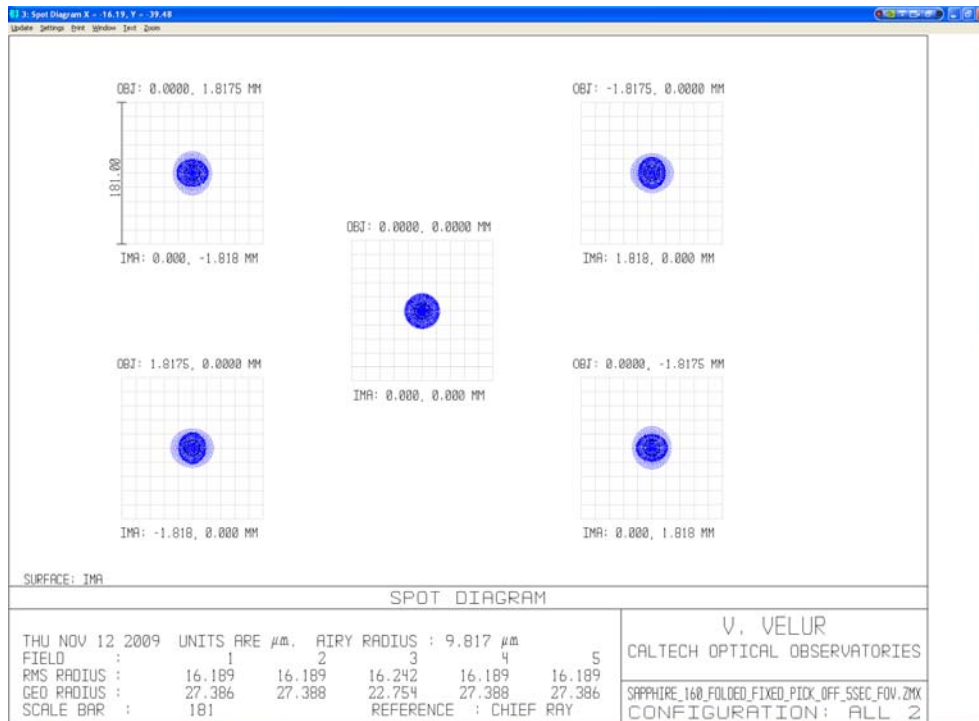


Figure 12 - Spot diagram showing the performance of the fixed LGSWFS pick-off over a 5 arcsec FoV (scale bar corresponds to 1/4 arcsec.).

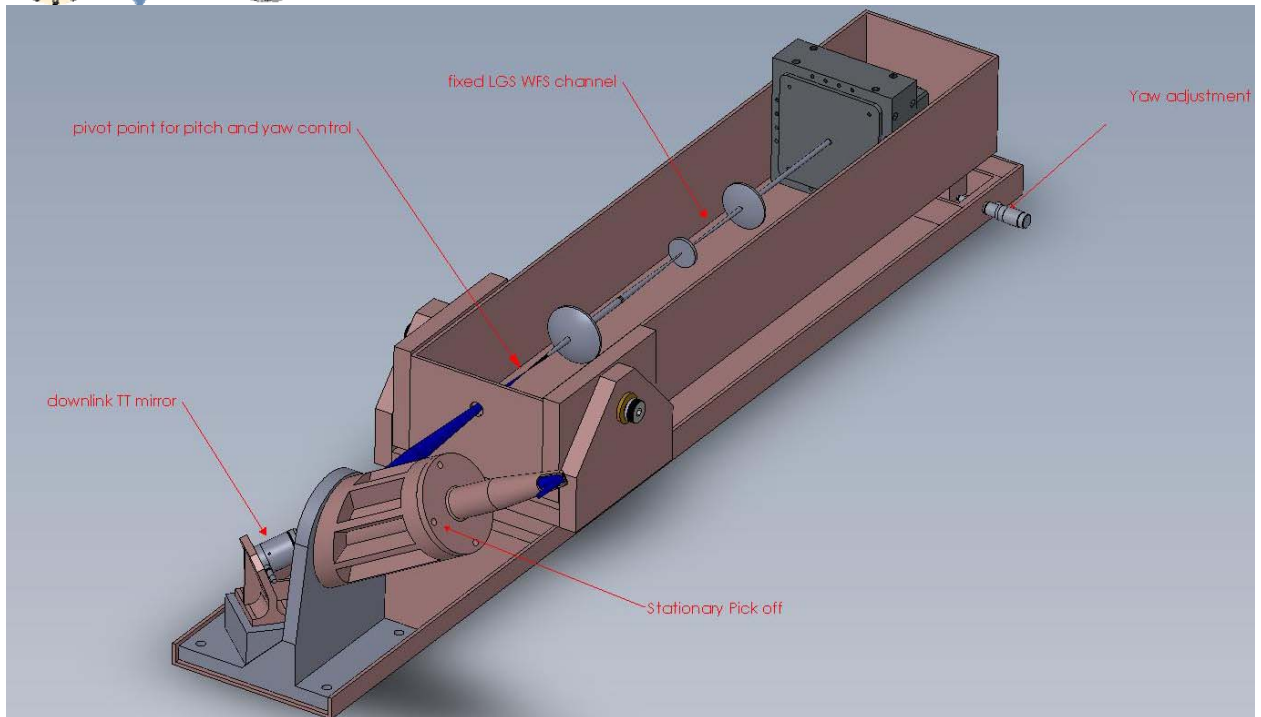


Figure 13 - Mechanical design of stationary fixed LGSWFS channel with stationary 1:1 pick-off relay with the downlink tip-tilt mirror at the relay's pupil location. Each tomo. LGSWFS is equipped with yaw and pitch motion, which along with the downlink TT mirror can be used to align each channel to the incoming beam and keep the lenslet to LODM registration.

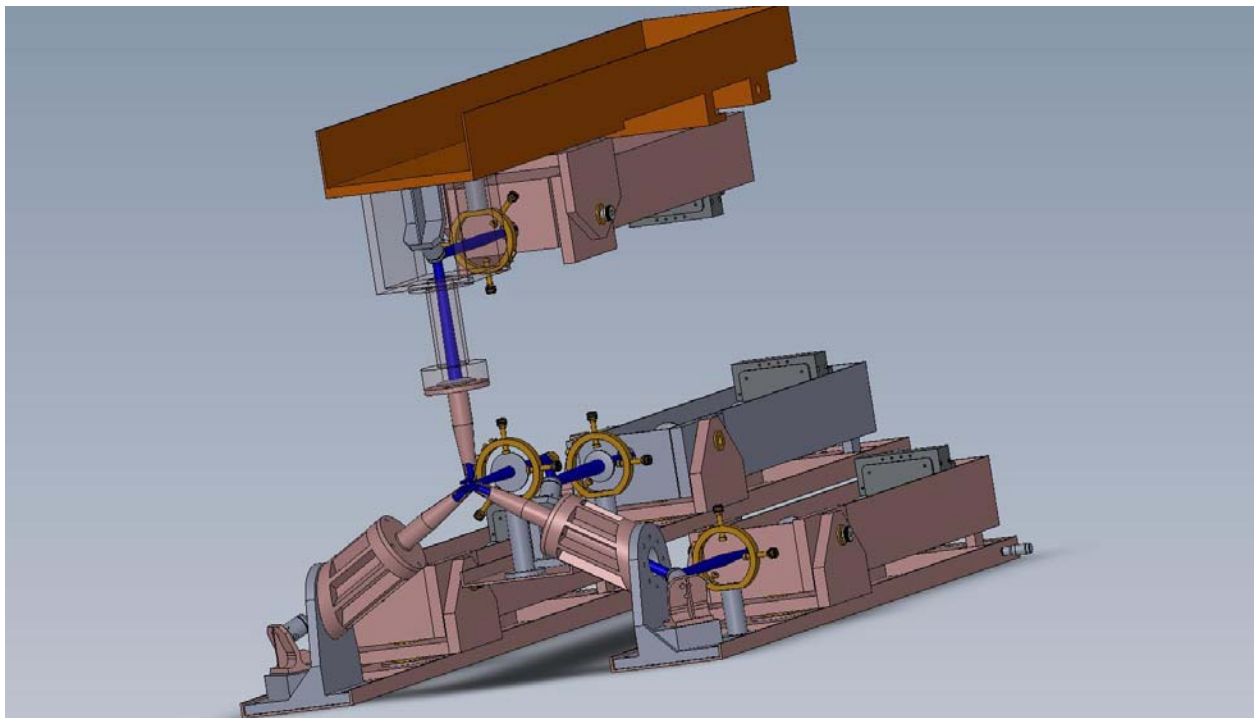


Figure 14 – Mechanical assembly of the fixed asterism pick offs and sensors assembly showing the 4 fixed LGSWFS's with one located in the middle and other three located equidistant from each other on a 10 arcsec circle about the central axis.



5.2.1.3. Fixed LGSWFS post-lenslet relay design and performance

To ensure that the requirement on the wavefront quality delivered by the WFS relay, the relay was modeled separately and the image quality of the relay assessed independently. The layout of the relay is shown in Figure 15. The relay delivers sub 1 μ m RMS spots with a 0.03% grid distortion at a demagnification of 0.89.

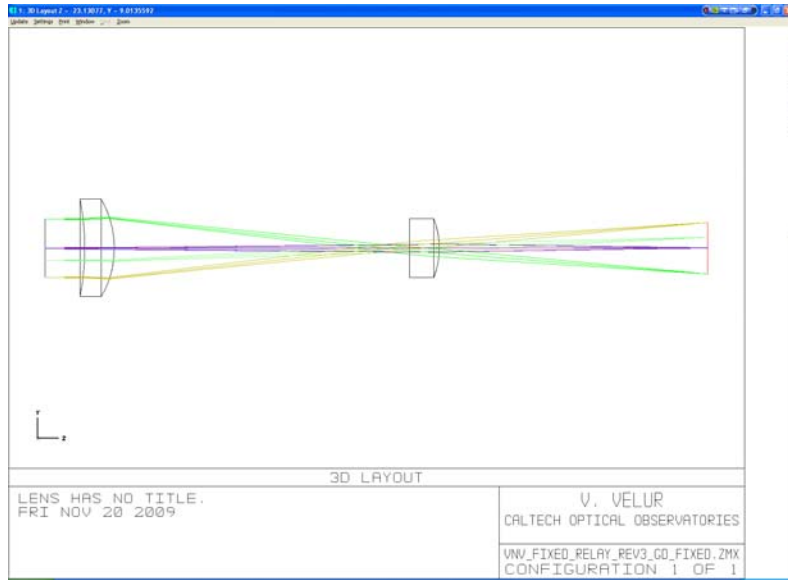


Figure 15 - fixed LGSWFS post-lenslet WFS relay layout.

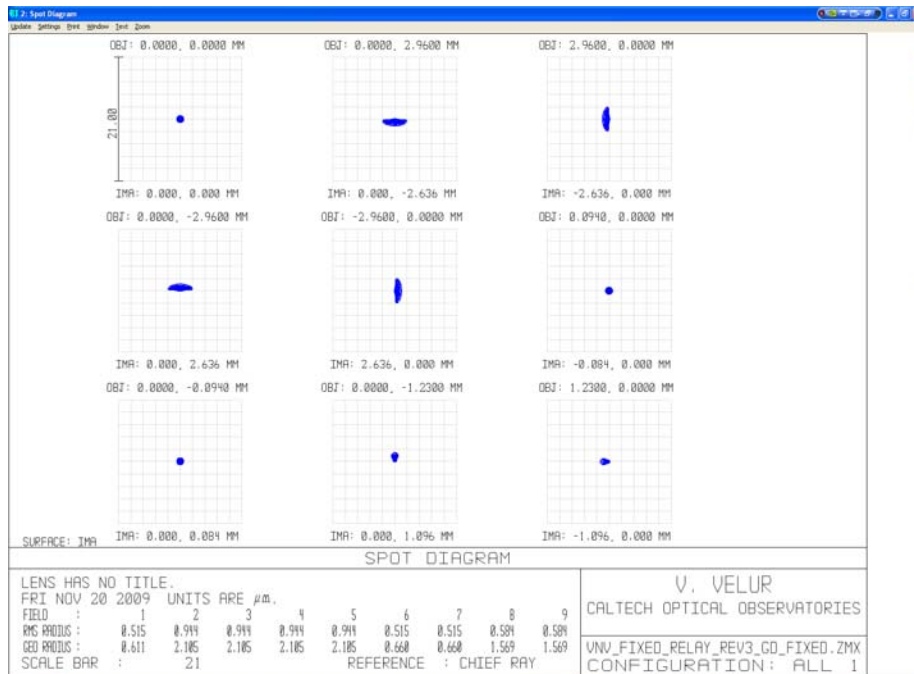


Figure 16 – Spot diagram showing an on-axis point and 4 extreme points of the lenslet spots with the worst case spot size being 0.95 μ m RMS radius. Detector pixel size is 21 μ m for reference. Field points 6 and 7 are one lenslet spot away indicating that the magnification is matched to 84 μ m spot separations at the detector. The grid distortion of the relay is 0.03%.



5.2.1.4. Fixed WFS design and performance

The fixed LGSWFS channels use a stock collimator, a custom lenslet and a set of 2 custom relay lenses. All optical components are singlets, giving rise to a total of 10 surfaces that need to be laser line coated at 589 nm. The transmission of this module is $(99.6\%)^{10} * 92.5\%$ (lenslet scatter losses) = 88.86%. The transmission of the system with the pick off (2 folds + 2 lenses) is $(99.6\%)^{16} * 92.5\%$ = 86.75%. The layout and the spot diagram from the WFS channel are shown in Figure 17 and Figure 18. The footprint diagram shown in Figure 19 indicates that the plate scale is accurate.



Figure 17 - layout of fixed LGSWFS, The total length of the sensor is 230 mm. The relay is composed of a best-form lens for a collimator, a custom lenslet array and a set of custom singlet relay lenses.

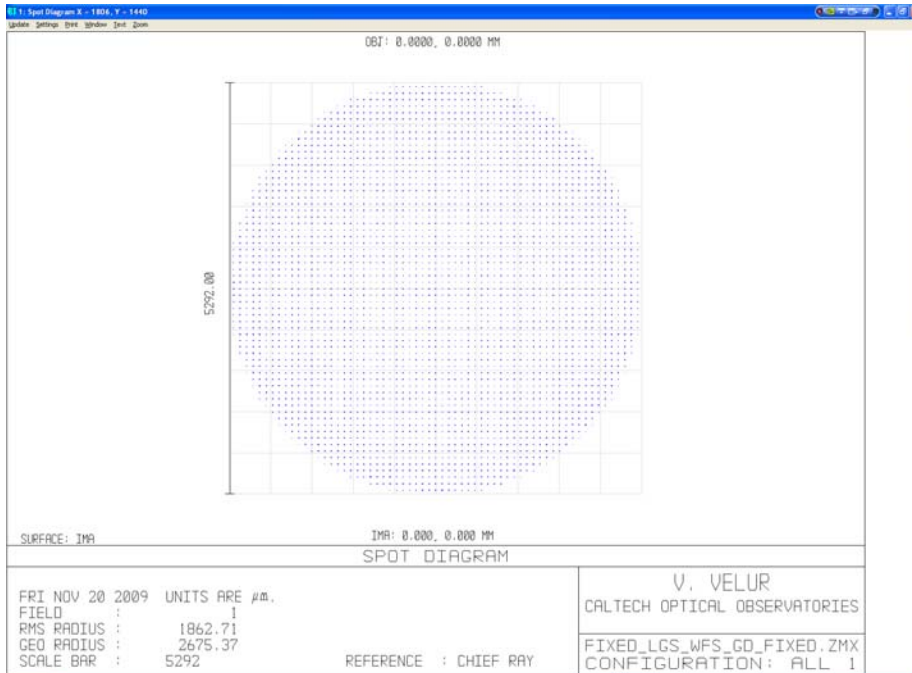


Figure 18 – fixed LGSWFS spot diagram showing 64x64 sub-apertures

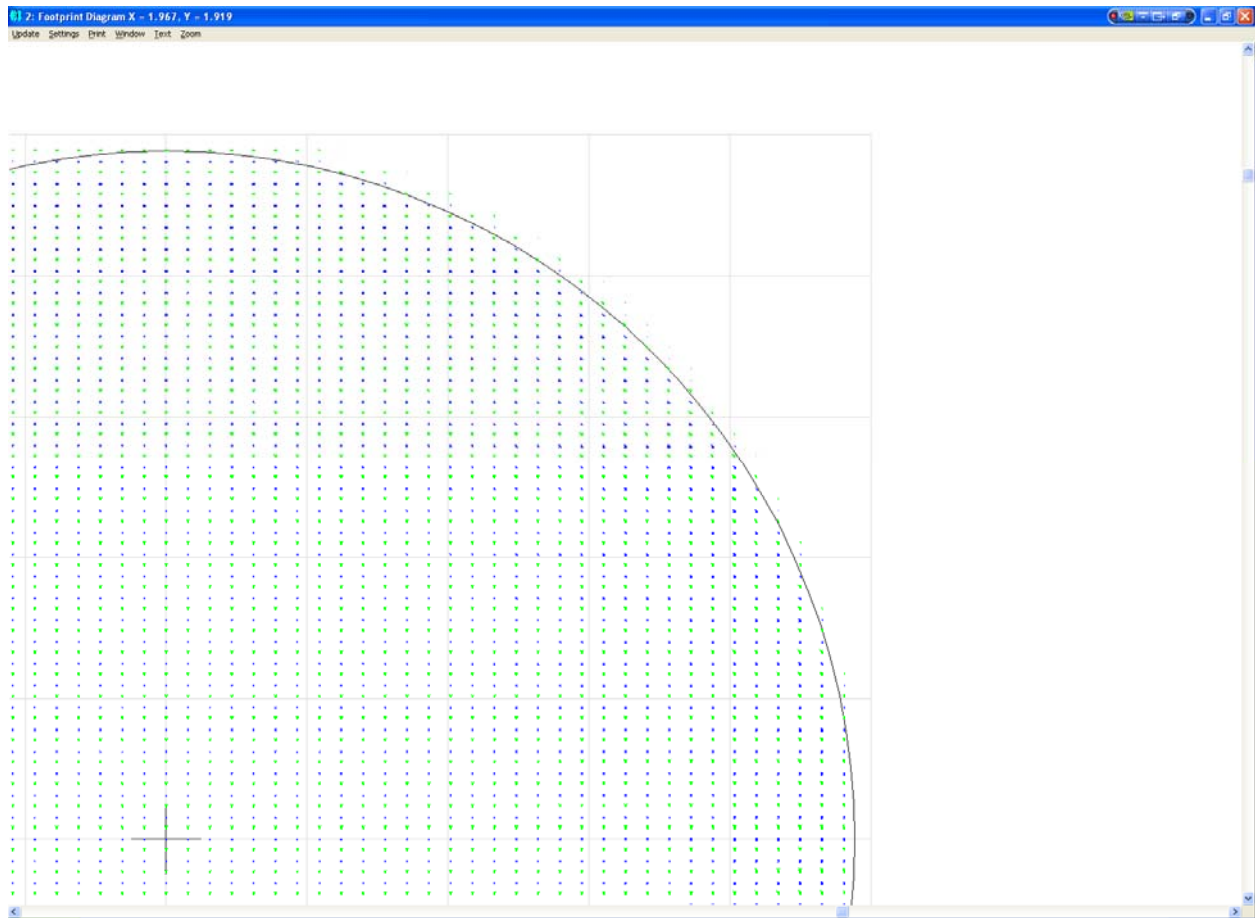


Figure 19 - footprint diagram with 2 field points, on on-axis point and one 1.41 arcsec (1205.7 um) away showing that the plate scale at the detector is 0 .705arcsec/pixel

5.2.2. Point and Shoot LGS WFS

5.2.2.1. Wavefront sensor design math

Pixel size/spot size =1.0 (as per Table 1)

Hence, 1.49" on sky corresponds to 21 um (detector has 21 um pixels).

$f_{\text{collimator}}/f_{\text{lenslet}} * 1/m = \text{Plate scale at the input of the sensor}(\text{um/asec})/ \text{Detector plate scale} (\text{um/asec})$

$$= 720 * 2 / 14.0939 = 102.171 \text{ (720 is the \# obtained from Zemax).}$$

$d_{\text{each lenslet}} = f_{\text{collimator}}/f\# * 1/(\# \text{ of sub-aps}) = 95/27.12 * (1/31) = 112 \text{ um}$

$m = 0.084/0.112998 = 0.74$, we choose $f_{\text{collimator}} = 95 \text{ mm EFL}$ from JML Optical's catalog.

$f2 = f_{\text{collimator}}/m * (29.78/720) = 95/0.74337 * (1/102.1714) = 1.25 \text{ mm (lenslet } f\# = 11.06)$

lenslet array Fresnel # = $(d_{\text{each lenslet}}/2)^2/(f*\lambda) = 4.33$.



Similar to the fixed LGS sensors, there exists a simple PnS LGSWFS with the least # of surfaces. The WFS will have a lenslet pitch of 84 μm and lenslet focal length of 0.69 mm with a 70.62 mm EFL collimator. The whole wavefront sensor is compact and has only 4 surfaces with either the collimator or the lenslet serving as the detector window. The sensor was designed and the design is available at: http://www.oir.caltech.edu/twiki_oir/pub/Keck/NGAO/WFS/PnS_lgs_wfs_norelay.ZMX.

5.2.2.2. PnS LGS pick off design and performance

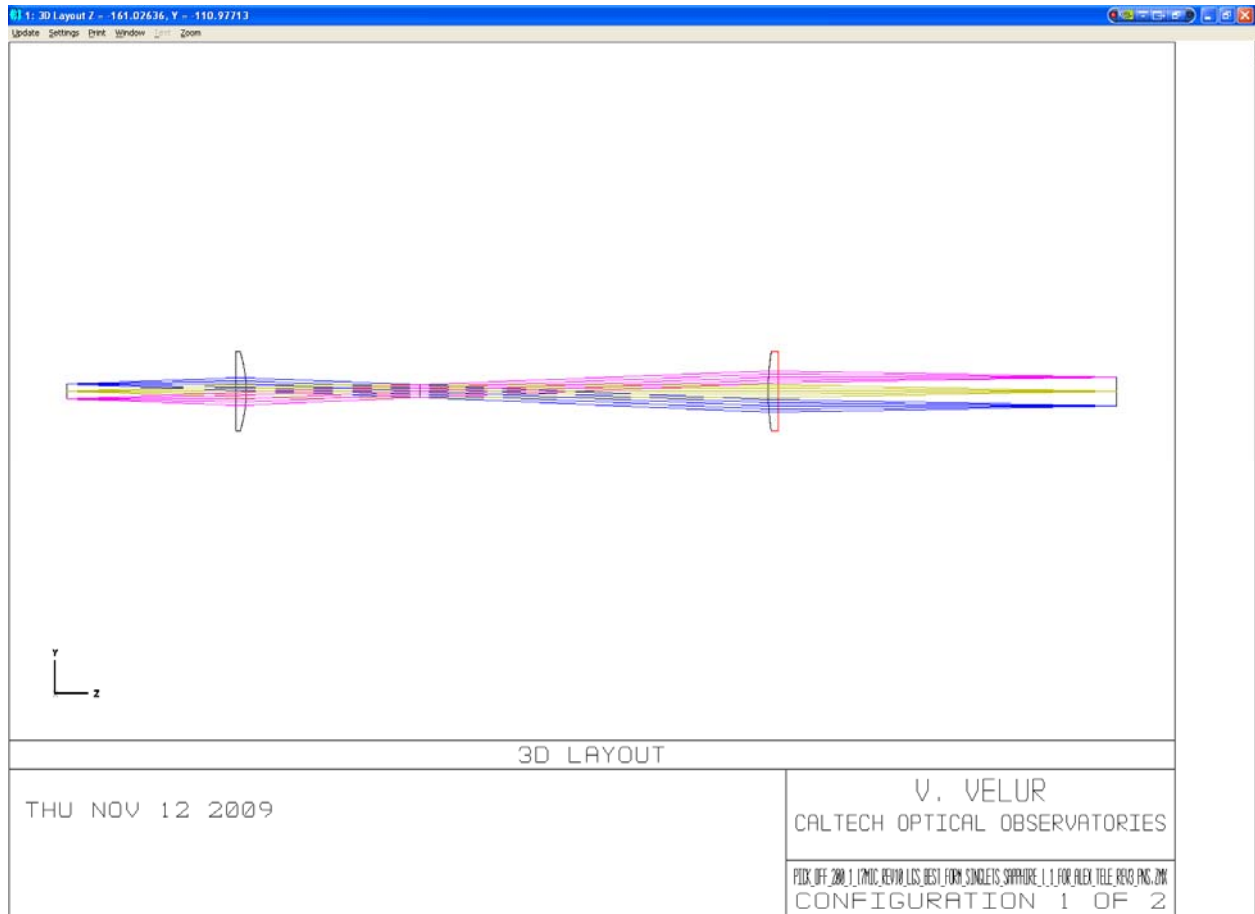


Figure 20 – Figure showing the telecentric unfolded layout of the PnS LGSWFS pick off. The relay is 1:2 due to packaging constraints.

A 1:2 telecentric relay was designed to accommodate mechanical packaging of the theta-phi pick-off and the fast TT mirror located at the relay pupil. The total length of the relay is 528 mm. Figure 21, Figure 22, Figure 23 show the spots from the relay and the mechanical assembly of the pick-off arm and the 3 channel PnS WFS assembly. The pick off mirror location is +10, -5 and -20 mm from the focal plane for the 3 PnS wavefront sensors. The light that is incident on the pick-off gets folded and collimated to form a pupil at fast TT mirror which folds the beam down to a pair of periscope mirrors. The pick-off mirror and the fast TT mirror are part of the rotatable lever and the periscope mirrors are part of a rotating crank. The combination of these two rotations facilitates positioning the pick-off anywhere in the field. There is a need to undo the combined effect of these rotations to keep the LODM pupil orientation fixed



onto the lenslet array. The design of the pick-off relay can be downloaded from http://www.oir.caltech.edu/twiki_oir/pub/Keck/NGAO/WFS/pns_pick_off.ZMX.

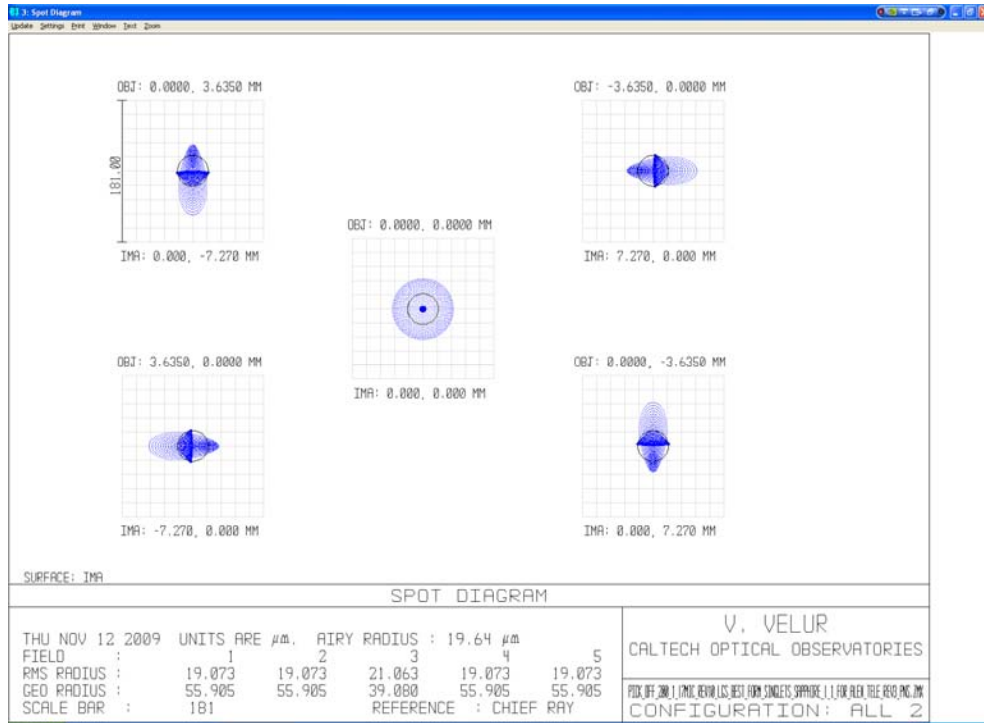


Figure 21 – Spot diagrams from the 1:2 Pns pick off relay showing spots with rms spot radius of 21 μm as compared to 130 μm rms spots delivered by the AO relay. For reference 101 μm is 1/4 arcsec.

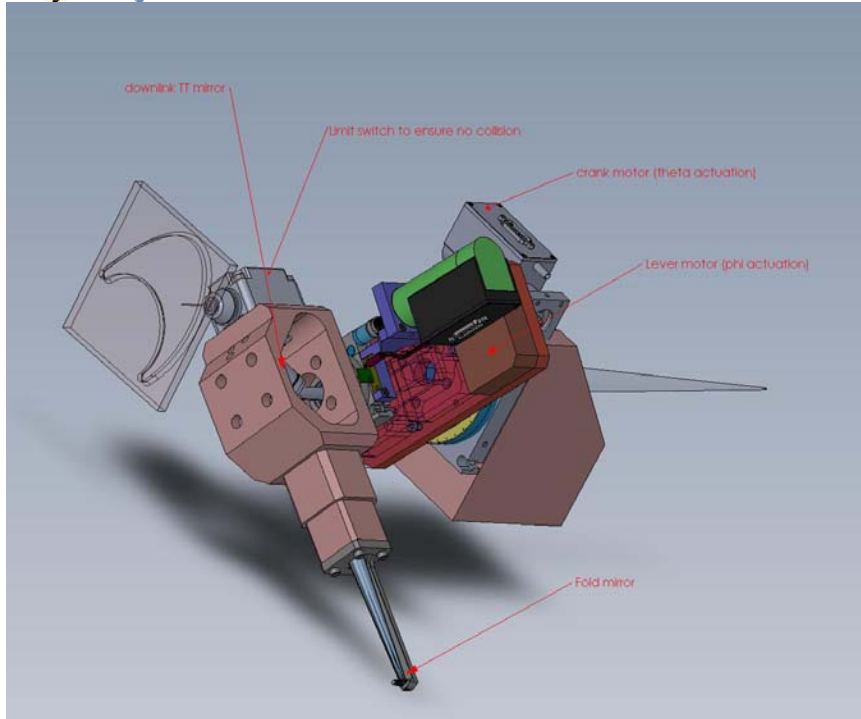


Figure 22 - mechanical assembly of a single deployable PnS pick-off showing the theta-phi mechanism with a downlink TT mirror located at the pupil. The blue and green parts are commercial motors that move the crank and lever.

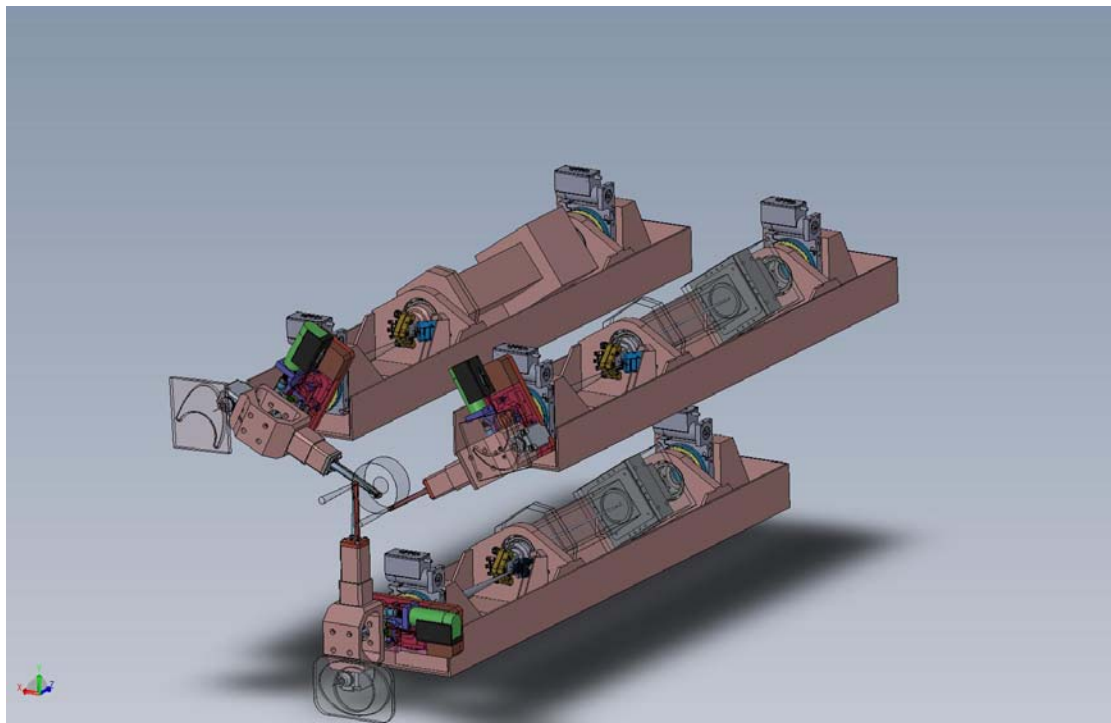


Figure 23 – Mechanical assembly of the PnS WFS channels showing the lenslet, the post-lenslet relay and the detector mounted on a bearing and a rotary stage to keep the lenslet and the LODM actuators registered with respect to each other



for any pick off position in the FoR. Each of the PnS WFS channel is also equipped with a TT mirror near the focus of the pick-off relay to keep the DM pupil registered onto the lenslet; this is necessary to eliminate pupil wander

5.2.2.2.1. PnS WFS Post-lenslet relay design and performance

The post lenslet relay was modeled separately for the PnS sensor and the performance of the relay measured. Since the lenslet spots are $f/11$ the design required doublets rather than just a pair of singlets. Models were built with single doublet and a singlet field lens with unsatisfactory performance. The 2 doublet relay gives sub um (RMS) spots with negligible grid distortion.

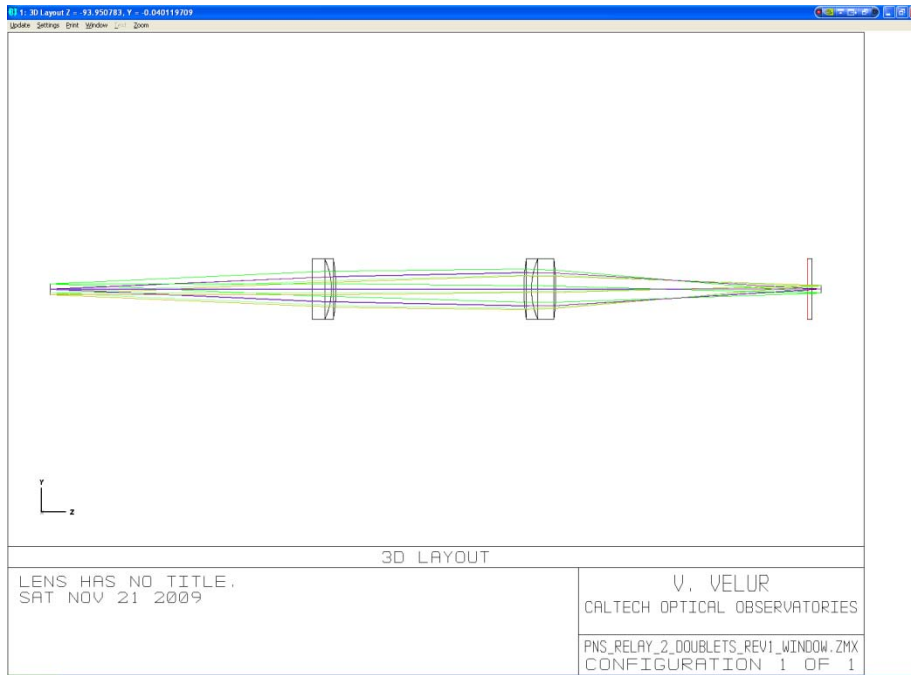


Figure 24 – Shows the layout of the post lenslet relay in the PnS LGSWFS, the length of the relay is 300 mm.

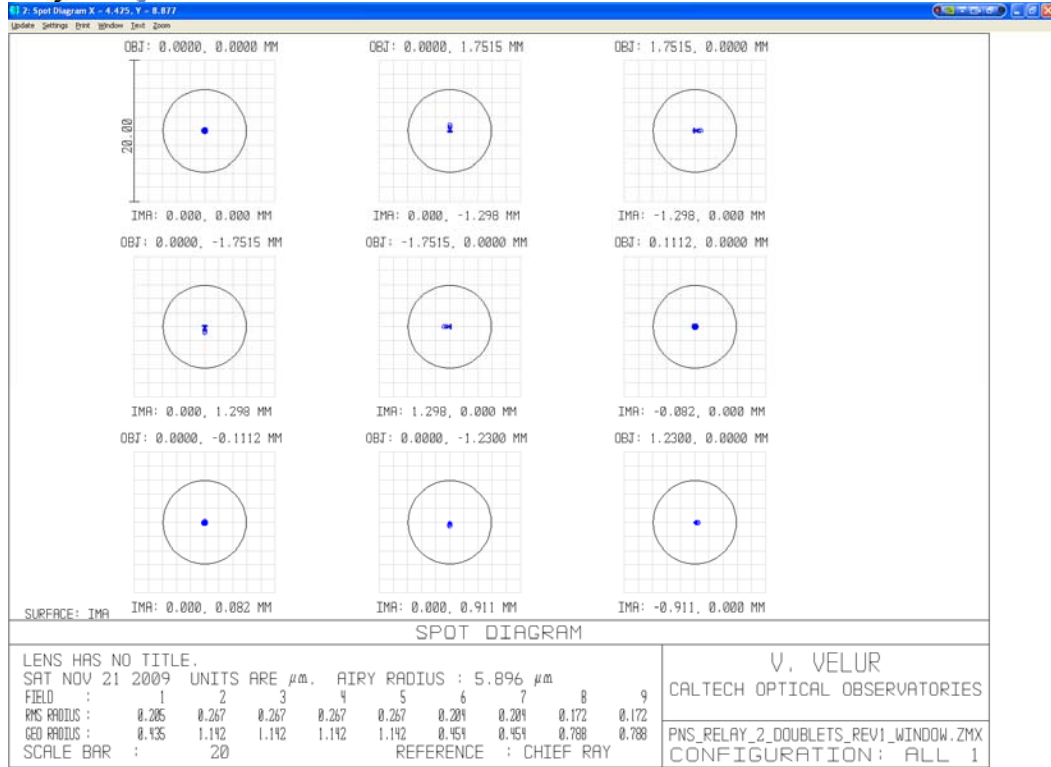


Figure 25 - Spot diagrams of the relay with on-axis and extreme field points. There are also 2 field points to indicate that the magnification is correct and 2 more located at $1/\sqrt{2}$ of the field size. The grid distortion of the relay is 0.001%.

5.2.2.2.2. WFS design and performance

The PnS WFS also uses a commercial best-form lens followed by a custom lenslet and relay lenses. The design of the WFS can be downloaded from: http://www.oir.caltech.edu/twiki_oir/pub/Keck/NGAO/WFS/PnS_lgs_wfs_doublets_rev1_window.ZMX. The WFS spots are shown in Figure 27 and a footprint diagram was used to verify the plate scale of the sensor. The total length of the sensor is 490 mm.

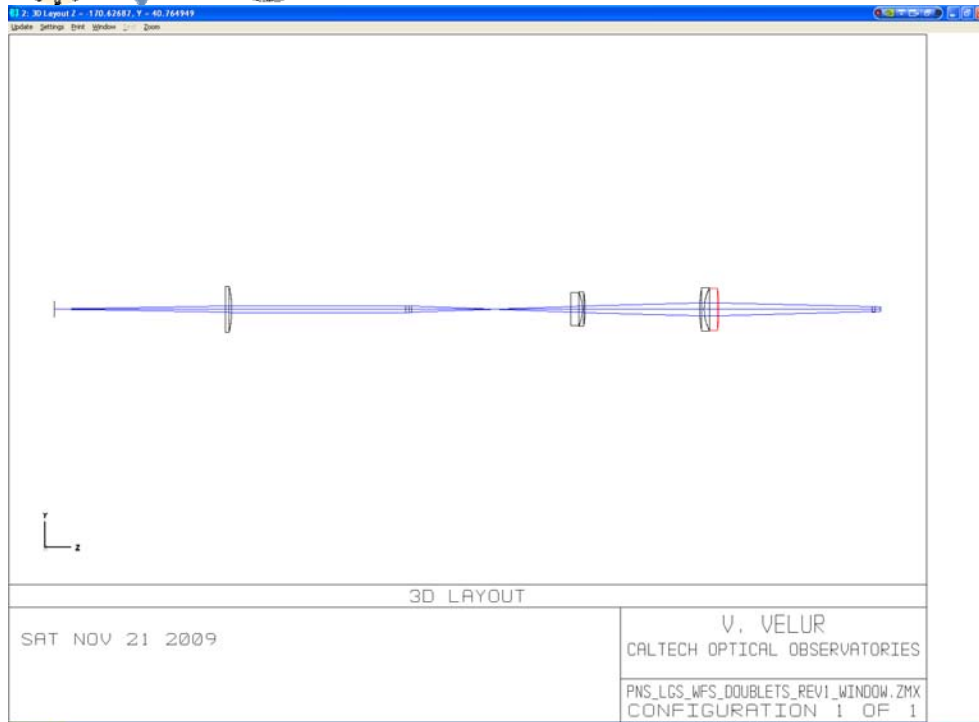


Figure 26- layout of the PnS WFS; the total length of the sensor is 490 mm. (I can make the relay longer to get better spots at the detector).

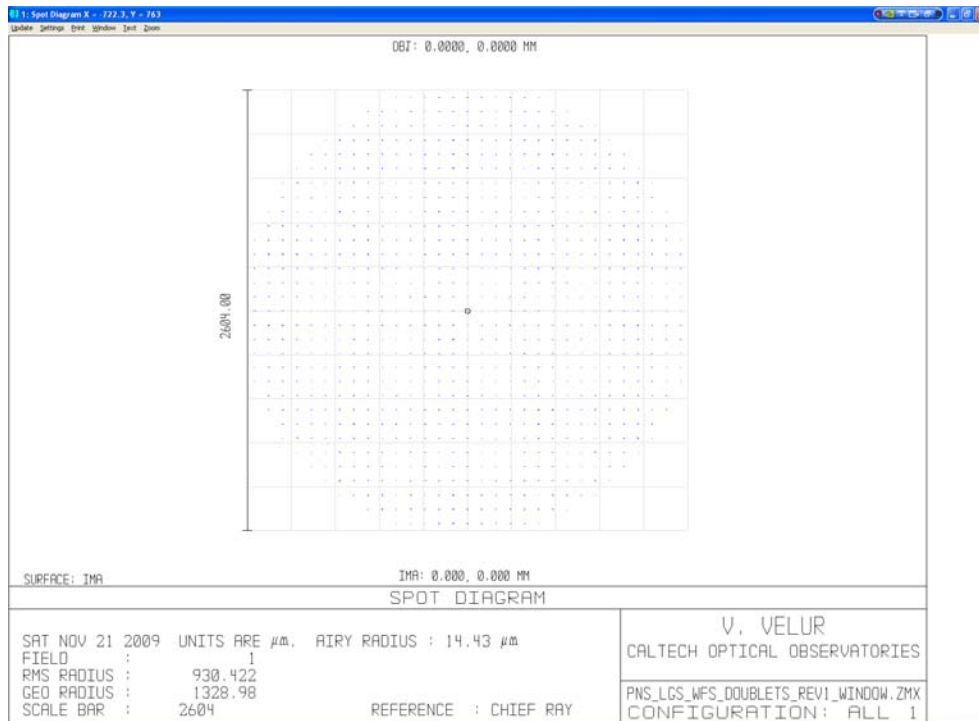


Figure 27 - spot diagram at the detector



5.2.3. Performance of the sensors with the A0 relay

6. Mechanical Design

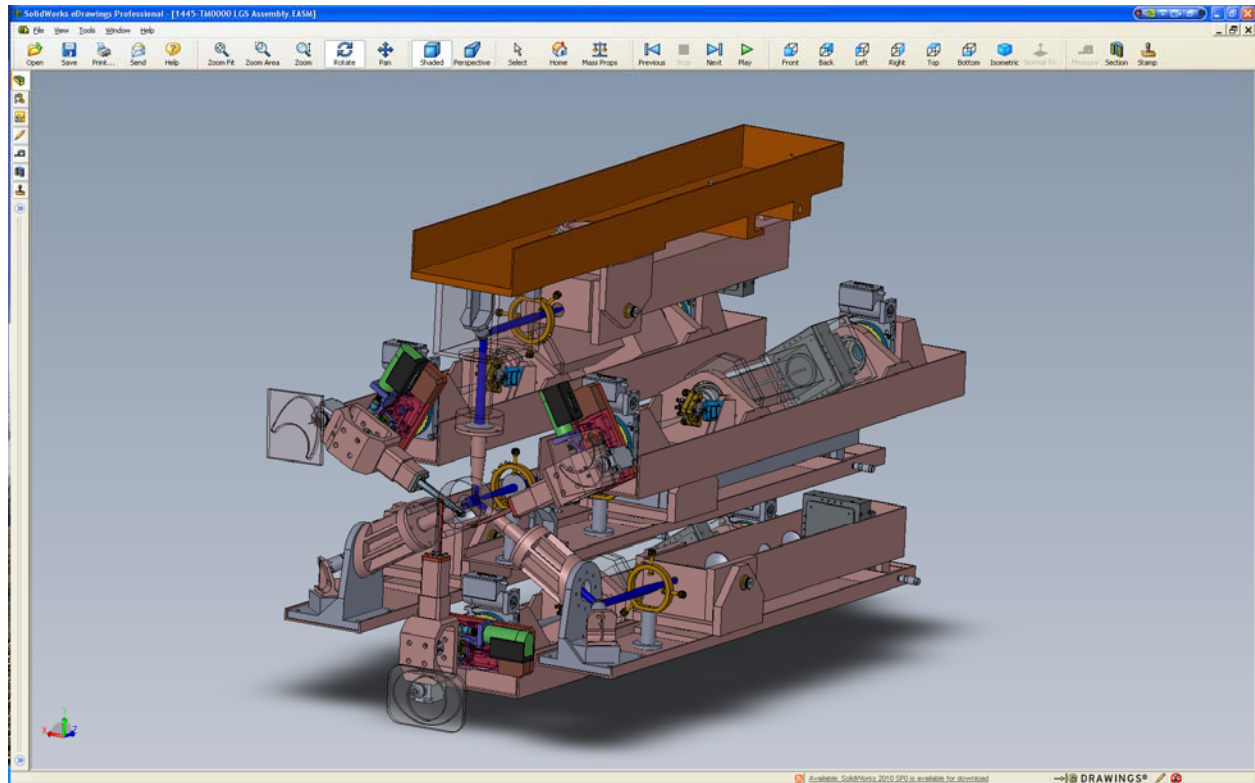


Figure 28 - mechanical assembly of the LGSWFS



6.1.1. Movable and stationary pick off design

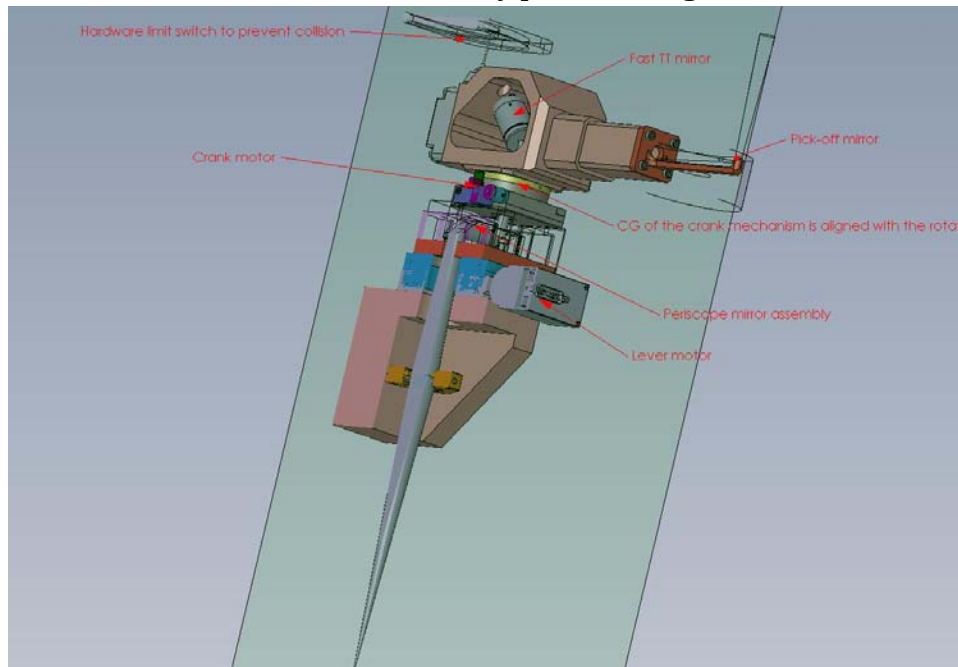


Figure 29 - part cross sectional view of the PnS pick-off

6.1.2. PnS relay mechanical design

6.1.3. Enclosure and linear stage

6.1.4. Pupil registration and TT corrector

Because the LGS light path to the WFS is not perfectly telecentric it is necessary to register the DM actuators and the lenslet for each point in the field for the PnS WFS (if the effect is not measured and calibrated). For this process we have a slow TT mirror near the pick-off focus to register the LODM actuators to the lenslet. We also provide a pitch and yaw mechanism to align the fixed LGS WFS lenslets to the LODM. Each LGS arm has a downlink TT mirror to correct the differential motion of LGS light WRT the science light at the pupil formed in the pick-off mechanism.

6.1.5. Hardware choice

7. Requirements compliance

8. Risk and risk mitigation plan

9. Work left to do

Stray light (including Rayleigh scatter) analysis -

ⁱ [KAON 644 - Build-to-Cost Architecture Wavefront Error Performance](#)



ii [Construction and testing of the wavefront sensor camera for the new MMT adaptive optics system, P. C. McGuire et. al.](#)